Natural Resources Canada | Ressources naturelles Canada

GEOMATICS CANADA
OPEN FILE 42

Characterization of apparent GPS ionospheric delay gradients over Canada

R. Ghoddousi-Fard

2018

Canada

GEOMATICS CANADA
OPEN FILE 42

Characterization of apparent GPS ionospheric delay gradients over Canada

R. Ghoddousi-Fard

2018

Permanent link: https://doi.org/10.4095/308444

This publication is available for free download through GEOSCAN (http://geoscan.nrcan.gc.ca/).

Recommended citation
Ghoddousi-Fard, R., 2018. Characterization of apparent GPS ionospheric delay gradients over Canada; Geomatics Canada, Open File 42, 11 p. https://doi.org/10.4095/308444

Publications in this series have not been edited; they are released as submitted by the author.

Characterization of apparent GPS ionospheric delay gradients over Canada

Reza Ghoddousi-Fard

Abstract

Differential GNSS augmentation systems require reliable knowledge of spatial and temporal variations of ionospheric effects on GNSS measurements. In addition, recent developments in Precise Point Positioning observation models can benefit from ionospheric constraints from nearby stations. This requires an understating of ionospheric delay spatial de-correlation under different ionospheric conditions.

In this study vertical ionospheric delays estimated from GPS stations in Canada and adjacent regions are employed for studying spatial and temporal ionospheric gradients during periods of quiet and disturbed ionospheric conditions. Ionospheric delay differences at each pair of ionospheric pierce points from different stations and satellites are used to characterize apparent spatial ionospheric gradients over the studied region. Temporal variations were also studied by differencing vertical ionospheric delays from the same satellite and station over specified periods.

Introduction

Performance of precise GNSS positioning can be affected by ionospheric irregularities. Differential ionospheric delays should be known or interpolated with a high precision, if carrier phase ambiguities need to be fixed for precise positioning. Recent developments in Precise Point Positioning observation models require improved information or capabilities to interpolate ionospheric delays. The relationship between ionospheric disturbances and error in ionospheric corrections for a rover receiver has been shown (see e.g. Hernandez-Pajares et al. [2006]). Walter et al. [2004] showed the effects of large ionospheric gradients on GPS wide and local area augmentation system users. Lee et al. [2006] reported standard deviations of vertical ionosphere gradients on the order of 1-3 mm/km for non-stormy ionosphere condition. In their analysis, they used stations in the United States region and suggested a standard deviation of 4 mm/km as a conservative ionosphere spatial de-correlation for nominal days.

In this study, we have used data sets of vertical total electron content (VTEC) estimated at ionospheric pierce points (IPP) being routinely used for TEC map generation over Canada and adjacent regions. These are used to compute apparent VTEC gradients in the Canadian region during quiet and moderately disturbed ionosphere periods.

Spatial and temporal gradients studied in this paper followed by data sets used in this study are introduced in the first two sections. Correlation of apparent gradients to geomagnetic

activity as well as challenges facing gradient calculation over short distances are discussed in the following sections. The last section is devoted to summary and conclusion.

Spatial and temporal VTEC gradients

In order to study spatial gradients, VTEC at IPP as estimated from a single layer model are differenced at pairs of IPPs within 500 km from all combinations of receivers and satellites at the same epoch. VTEC difference from mixed receivers and satellites can be written as:

$$VTEC(\vec{X}_j,t)-VTEC(\vec{X}_i,t)=m_{r_j}^{s_j}{}^{-1}.\left(\phi_{L^j}-\delta_{r_j}-\delta^{s_j}\right)-m_{r_i}^{s_i}{}^{-1}.\left(\phi_{L^i}-\delta_{r_i}-\delta^{s_i}\right)+\varepsilon_{ij} \quad (1)$$

where $\vec{X}_i$ ($\vec{X}_j$) is the position vector of first (second) IPP, t is the epoch of measurement, ϕ_{L^i} (ϕ_{L^j}) is the phase-levelled observable at first (second) IPP, $m_{r_i}^{s_i}$ ($m_{r_j}^{s_j}$) is the first (second) mapping function converting slant TEC to VTEC, δ_{r_i} and δ_{r_j} are respective receiver differential code biases (DCB), δ^{s_i} and δ^{s_j} are respective satellite DCB; and ε_{ij} is the noise and multipath effects on the VTEC difference.

It is noted from equation (1) that in addition to noise and multipath, VTEC difference is also affected by uncertainties in mapping functions, code smoothing (phase-levelling) and receiver and satellite differential code biases.

Temporal gradients are studied using IPPs observed by the same receiver and satellite during periods of up to 4 hours. The equation for VTEC differenced over epoch t_i and t_j can be written as:

$$VTEC(\vec{X},t_j)-VTEC(\vec{X},t_i)=m_{t_j}{}^{-1}.\phi_{L^j}-m_{t_i}{}^{-1}.\phi_{L^i}+\varepsilon_{ij} \quad (2)$$

where parameters are similar to those introduced in equation (1). One may note that uncertainties in satellite and receiver DCBs are removed from equation (2) by assuming that they are constant over the differencing period. However, while satellite DCBs are rather stable over long periods (see e.g. Sardón and Zarraoa [1997]), sub-daily variation of receiver DCBs can be significant (see e.g. Ciraolo et al. [2007]).

Space (time) differenced VTEC values are divided by IPP separation distance (time) to derive spatial and temporal gradients. Due to the contribution of estimation errors in both types of gradients, they are referred to as apparent gradients.

VTEC data sets

In this study, a database of estimated VTEC used for routine VTEC map generation over most of North America [Ghoddousi-Fard et al., 2011] is employed for studying VTEC gradients. All possible pairs of IPP within 500 km distance observed every 5 minutes from about 75 stations in a defined region of *lat* > 40º and -150º < *lon* < -30º are used for differencing VTEC values. An elevation cut-off angle of 30º is used to minimize the effect of multipath and noise. Figure 1 shows, as an example, all IPPs in the studied region for March 17, 2013. Highest VTEC values are plotted in TEC unit (TECU) on the top layer of Figure 1 to help visibility of colors (i.e. only maximum values are visible in each pixel).

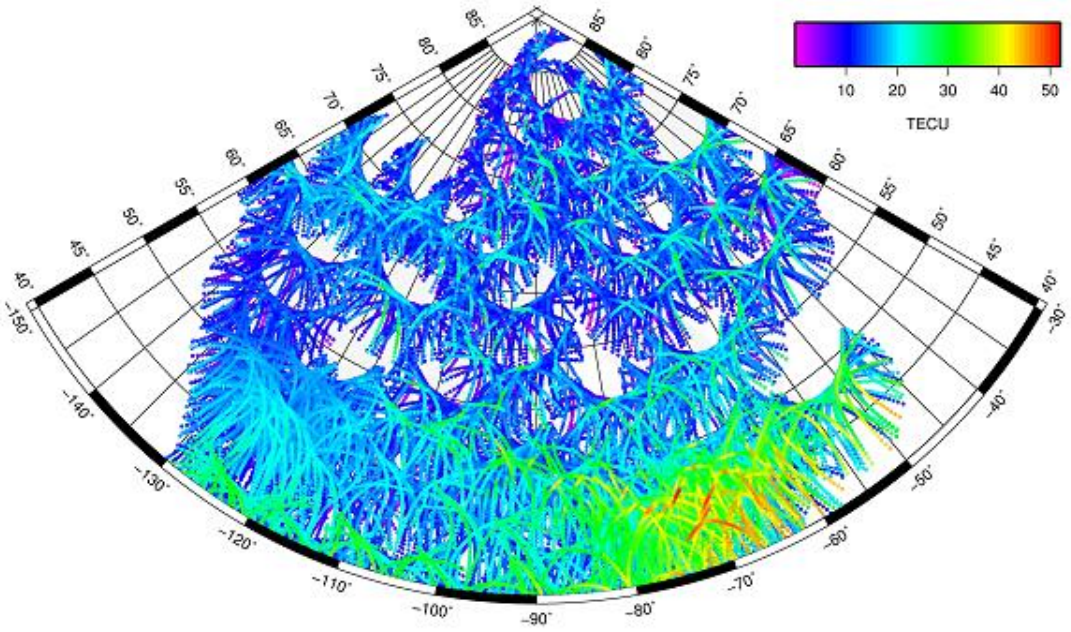

Figure 1 – VTEC at IPPs observed every 5 minutes during March 17, 2013 over *lat* > 40º and -150º < *lon* < -30º; elevation cut-off: 30º.

VTEC difference from all possible pairs within 500 km distance every 5 minutes in bins of 10 km by 1 TECU during a quiet day (January 2, 2013) and a disturbed day (March 17, 2013) are shown in Figure 2 as examples. As noted in Figure 2, compared to the quiet day, VTEC differences are increased during disturbed day, with the largest VTEC differences occuring over largest IPP separation distances. Also seen in Figure 2 is the distribution of IPP pair distances (IPP number in each bin) in the data sets used.

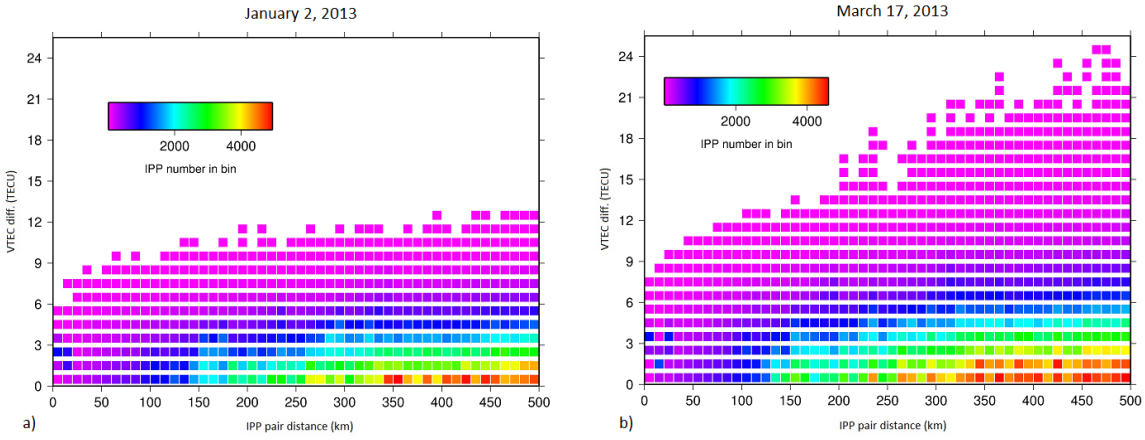

Figure 2- VTEC difference between all pairs of IPPs within 500 km in the studied region shown in bins of 10 km by 1 TECU during a) January 2, 2013; and b) March 17, 2013.

Apparent VTEC gradients response to geomagnetic activity

Characterization of spatial and temporal gradients is carried out using VTEC data from eight days during March 2012 to March 2013 with different levels of geomagnetic activities. The selection of days was such that to include most disturbed days during mentioned period as well as few arbitrarily chosen quiet days. The 3-hourly Kp index as provided by the World Data Center for Geomagnetism (http://wdc.kugi.kyoto-u.ac.jp/) are averaged daily and provided in Table 1 for the selected days. Real-time hourly equatorial disturbance storm time (Dst) index values as provided by the same data center are also plotted for each day in the last column of Table 1. Both indices are global indicators of the state of the Earth's geomagnetic activity. Figure 3 shows empirical cumulative distribution function (ECDF) of apparent spatial and temporal gradients calculated from VTEC differences during the selected days.

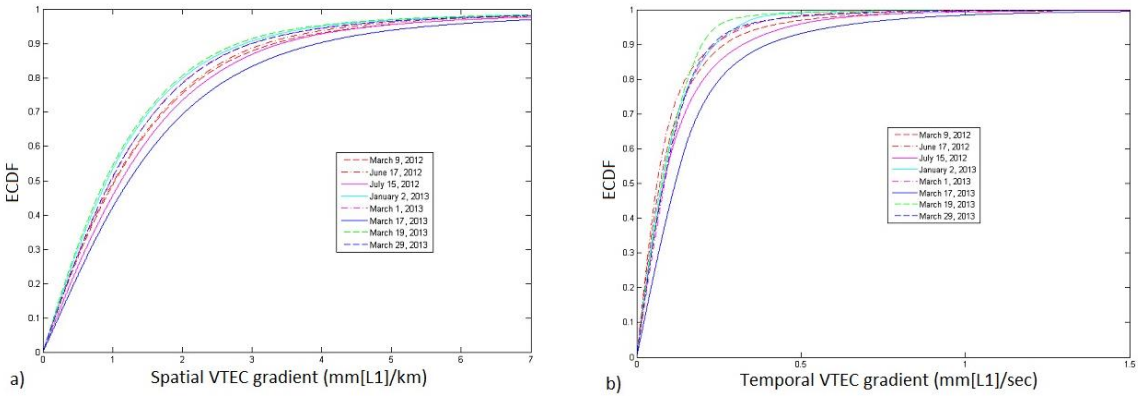

Figure 3- ECDF of apparent VTEC gradients during studied days: a) spatial, b) temporal.

Table 1 – Spatial and temporal apparent vertical ionospheric delay gradients on L1.

Date	Spatial (mm/km)			Temporal (mm/sec)			Daily mean 3-hourly Kp index	Real-time hourly equatorial Dst Plot
	95th percentile	Mean	Std	95th percentile	Mean	Std		
March 9, 2012	**4.71**	**1.64**	**2.54**	**0.39**	**0.12**	**0.18**	**5.50**	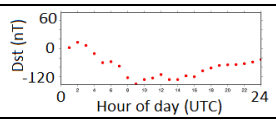
June 17, 2012	4.43	1.58	2.38	0.33	0.10	0.14	4.60	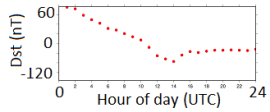
July 15, 2012	**4.76**	**1.71**	**2.53**	**0.46**	**0.14**	**0.19**	**5.83**	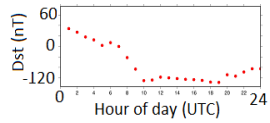
January 2, 2013	3.99	1.45	2.43	0.31	0.11	0.12	0.67	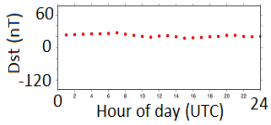
March 1, 2013	4.23	1.51	2.37	0.32	0.12	0.14	4.38	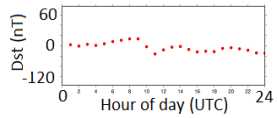
March 17, 2013	**5.52**	**1.91**	**2.77**	**0.60**	**0.18**	**0.25**	**5.25**	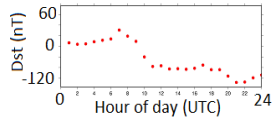
March 19, 2013	3.88	1.38	2.15	0.24	0.10	0.10	1.17	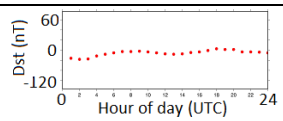
March 29, 2013	4.19	1.50	2.34	0.31	0.11	0.14	3.92	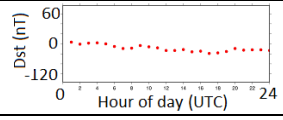

Figure 4 shows 95th percentile of both temporal and spatial gradients plotted against daily mean Kp index. It is noted that during days with daily mean 3-hourly Kp index exceeding 5 (moderately disturbed periods when also disturbances of Dst occurred with large negative values), 95th percentile of spatial apparent vertical ionospheric delay gradients (see also Figure 3) were exceeding 4.5 mm/km. The 95th percentile of temporal gradients during the same days were also larger than the other studied days (near and exceeding 0.5 mm/sec). Mean and standard deviation of daily spatial gradients during all studied days are above 1 and 2 mm/sec respectively. These are reaching close to 2 and 3 mm/sec respectively during geomagnetically active days.

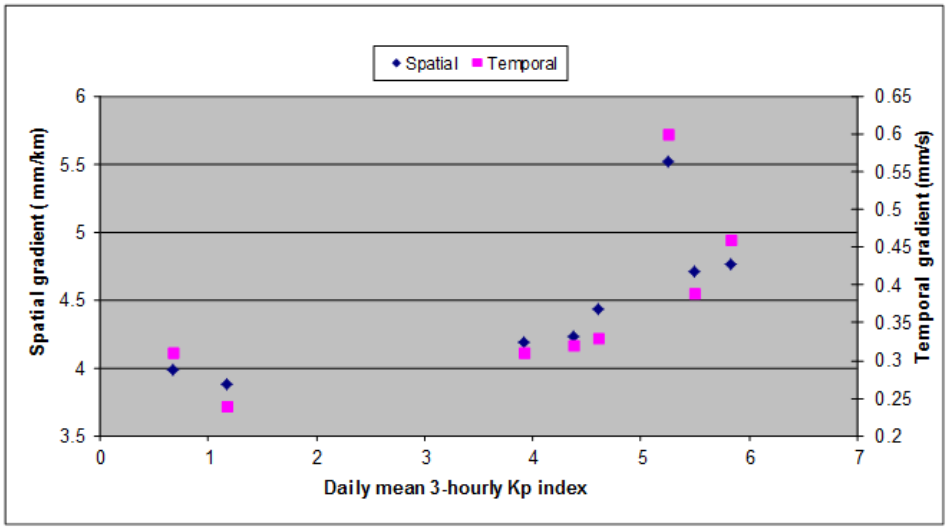

Figure 4- 95th percentile of spatial and temporal gradients vs. daily mean 3-hourly Kp index.

One should note that while Kp and Dst indices as global indicators of geomagnetic activity are not specific to the studied region, the statistics of the gradients are still sensitive to them. However, one should consider the contribution of VTEC estimation errors on the resulted gradients. Considering the elevation cut-off angle of 30^{o} used in this study, the effects of mapping function, noise and multipath errors are likely to be less significant compared to levelling error which remains to be the main adverse factor. Ciraolo et al. [2007] studied phase-levelling errors and reported errors varying from 1.4 to 5.3 TECU. In addition, sub daily variations of receivers' DCB may contribute to the VTEC estimates and consequently to the resulted gradients.

As seen in Table 1 and plotted in Figure 5 statistics of temporal and spatial gradients are highly correlated and as noted before both are responding to global geomagnetic activity. While temporal gradients are less susceptible to VTEC estimation errors (compare equations (1) and (2)), it is important to note the effect of IPP velocity on temporal gradients. The IPP velocity depends on satellite elevation angle and ionospheric shell height. As an example, IPP velocities studied at the same day and region plotted in Figure 1 are shown in Figure 6. It is noted that over the studied region, on a shell height of 450 km, and with an elevation cut-off angle of 30 degrees, IPP velocities varies from about 59 to 196 m/sec with a mean value of 98.2 m/sec. In presence of ionospheric disturbances caused e.g. by travelling ionospheric disturbances (TID) one should consider the Doppler effect caused by the relative movement between the satellite, ionospheric irregularity and it's altitude [Hernandez-Pajares et al., 2006]. The amount of this effect depends on the velocity and direction of the TID relative to those of the IPP. It is expected to be maximized when the direction of the TID and IPP are parallel and zero when the directions of the two are perpendicular.

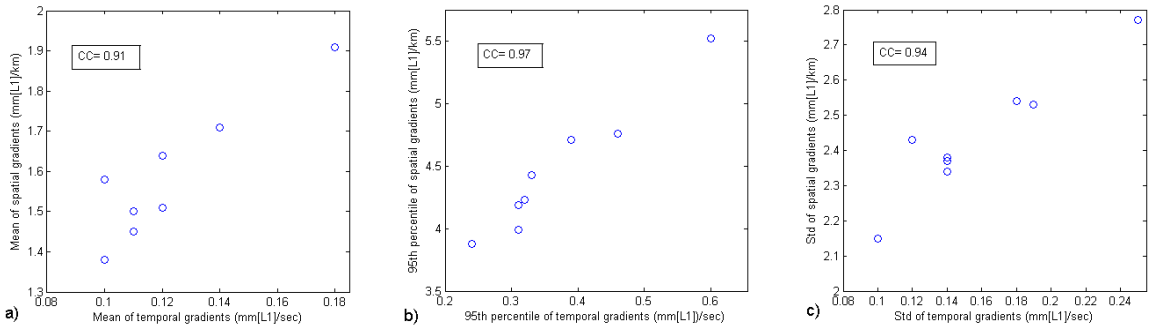

Figure 5- Correlation coefficient of statistics between temporal and spatial gradients: a) Mean, b) 95th percentile, and c) Std.

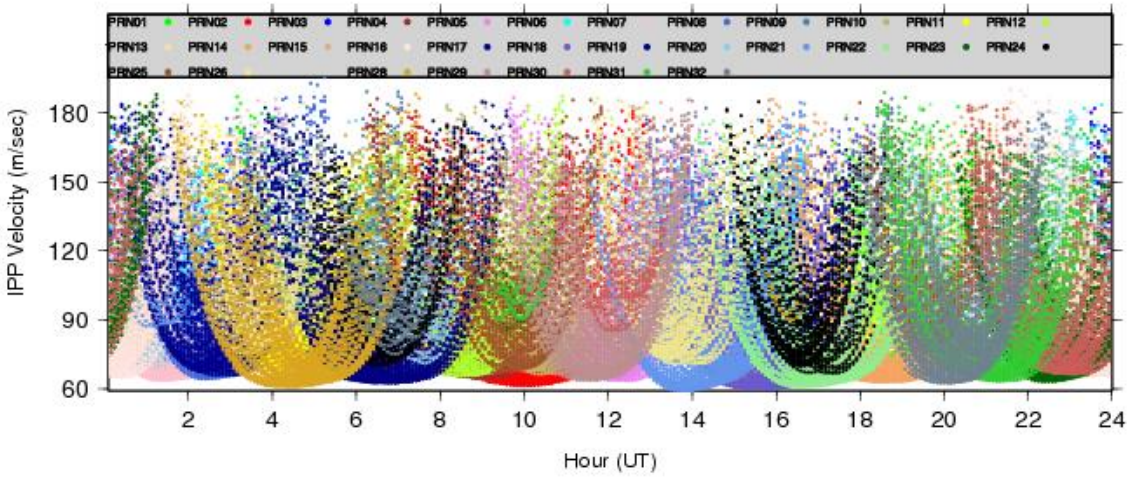

Figure 6- Velocity of all IPPs at a shell height of 450 km observed every 5 minutes during March 17, 2013 over lat > 40º and -150º < lon < -30º; elevation cut-off: 30º.

Short distance gradients: a challenge

Looking at the bin with the shortest distances (0-10 km) and dividing it into bins of 2 km, VTEC difference statistics are calculated and summarized in Table 2. No clear dependency of values to geomagnetic activity can be concluded from the resulting statistics. Also there is no clear dependency of VTEC differences to the bin IPP pair distance. It is also worth mentioning that sample sizes in bins are considerably different, which may affect statistics. In Table 2, values resulting from sample sizes of more than 700 are noted by bold font while other values are resulting from sample sizes of less than 80. A standard deviation of about 0.6-0.7 TECU noted where large sample sizes (>700) are used for statistics.

Table 2- VTEC difference statistics at IPPs with distances up to 10 km, divided in 2 km bins. Unit: TECU

IPP pair distance range (km)	[0-2)		[2-4)		[4-6)		[6-8)		[8-10)	
Date	Mean	Std	Mean	Std	Mean	Std	Mean	Std	Mean	Std
March 9, 2012	3.66	0.78	**4.55**	**0.78**	2.36	2.00	2.71	2.42	2.56	2.08
June 17, 2012	2.56	2.70	3.13	3.01	2.43	2.02	2.80	2.34	2.52	2.06
July 15, 2012	2.54	1.09	**3.19**	**0.60**	2.59	1.79	2.47	1.72	2.33	1.92
January 2, 2013	2.03	0.64	**2.55**	**0.57**	2.03	1.68	2.85	2.14	2.36	1.71
March 1, 2013	**3.90**	**0.65**	2.65	2.24	2.32	1.93	2.22	1.49	2.44	1.96
March 17, 2013	2.80	1.01	**3.37**	**0.62**	3.00	2.15	2.96	2.35	3.41	2.80
March 19, 2013	4.06	0.74	**3.17**	**0.55**	1.92	1.52	2.39	2.01	2.44	1.98
March 29, 2013	**3.92**	**0.68**	**3.64**	**0.67**	2.26	1.61	2.50	1.79	2.26	1.65

As can be seen in Figure 7 there is a mean RMS VTEC difference of about 3-3.5 TECU in selected bins over the studied days. This value may be assumed as a nominal VTEC estimation uncertainty. Assuming no correlation between VTEC estimates at two IPPs, a nominal VTEC difference error of $\sqrt{2}\times 3$ TECU is assumed. The effect of this nominal value on resulted vertical ionospheric delay gradients on L1 is shown in Figure 8. It is clear that over short IPP separation distances, the contribution of VTEC estimation errors on spatial gradients is significantly increased. Therefore a proper assessment of spatial ionospheric delay gradients over short distances is a challenging task. Although some procedures may be employed to reduce the large effect of VTEC differences on short distances [Lee et al., 2006] by comparing and removing mean difference of continuous arcs of slant TEC measured by nearby stations; justification of such approaches may need detailed information of the ionospheric irregularities including TID moving faster than 0.3 km/sec (large-scale) and moving 0.05-0.3 km/sec (medium-scale) [Jacobson et al., 1995]. This is especially more challenging in Canadian region with a dynamic high-latitude ionosphere and ionization gradients that may be formed between the auroral and the mid-latitudes [Hunsucker and Hargreaves, 2003].

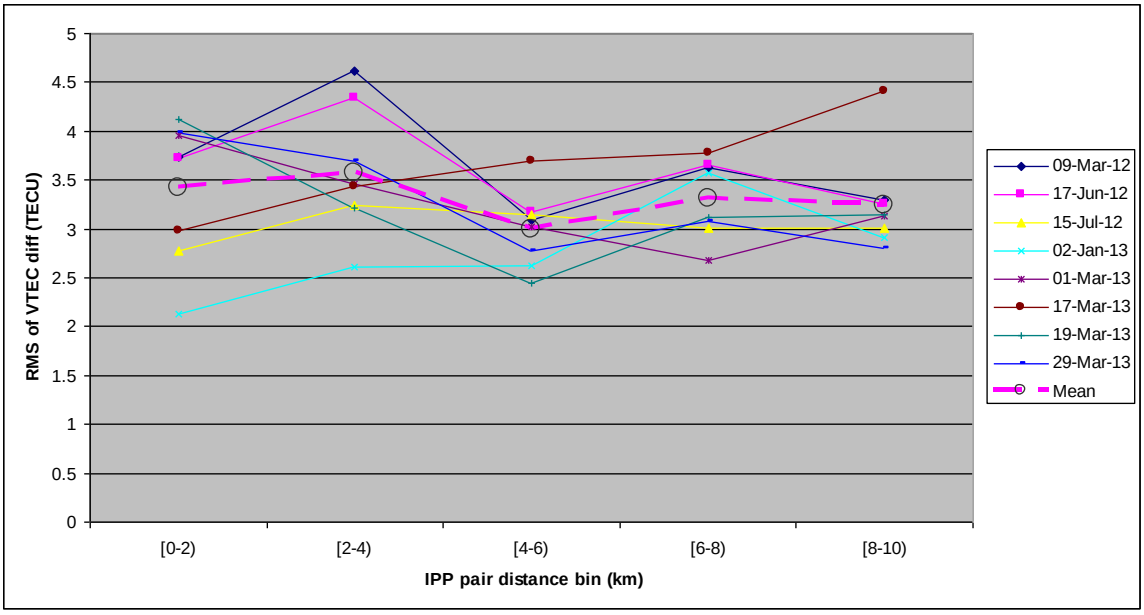

Figure 7– RMS of VTEC difference of IPP pairs separated up to 10 km in 2 km bins.

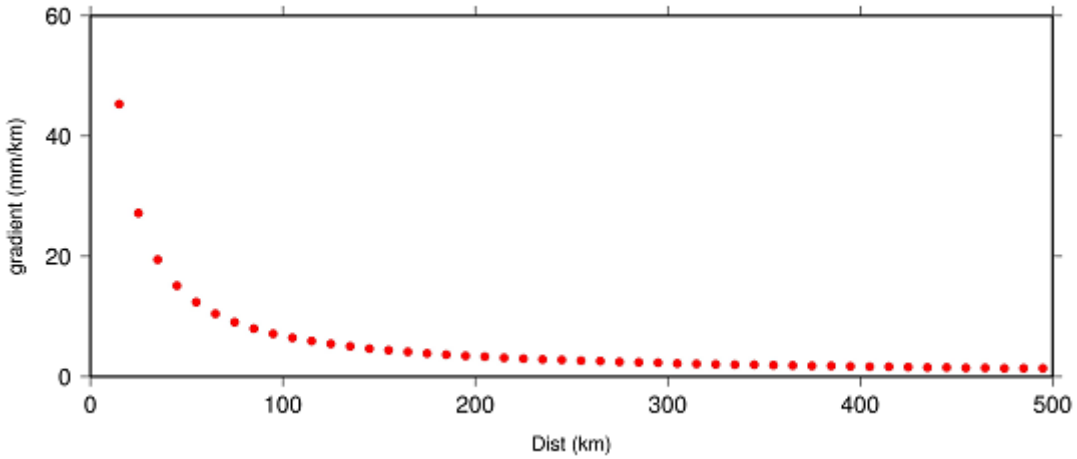

Figure 8– Apparent vertical ionospheric delay gradient on L1 as a result of a nominal (3 TECU) error per VTEC.

Using actual data for March 9, 2012 (a disturbed day already used in this study), mean and standard deviation of gradients in bins of 10 km IPP separation distances are plotted in Figure 9, together with sample size in each bin. As noted, large gradients over short distances is due to the degradation of results because of VTEC estimation uncertainties. However, distribution of IPPs in this study is such that sample number increases with increasing the IPP pair separation distance. This minimizes the effects of the large gradients (caused by short IPP separation distances) on overall statistics provided in Table 1. In all spatial (temporal) gradient statistics reported in this paper a rejection criterion of 100 mm/km (10 mm/sec) is considered. This criterion rejects a considerably large number of samples in short IPP separation distances for spatial gradient statistics. For example, in a 5 km IPP separation distance only VTEC differences of up to 3.09 TECU are tolerated. This value is decreased to 0.62 TECU for IPP separation distances of 1 km. On the other hand,

this criterion e.g. tolerates VTEC differences of up to 123.5 TECU in an IPP separation distance of 200 km which practically means no rejection!

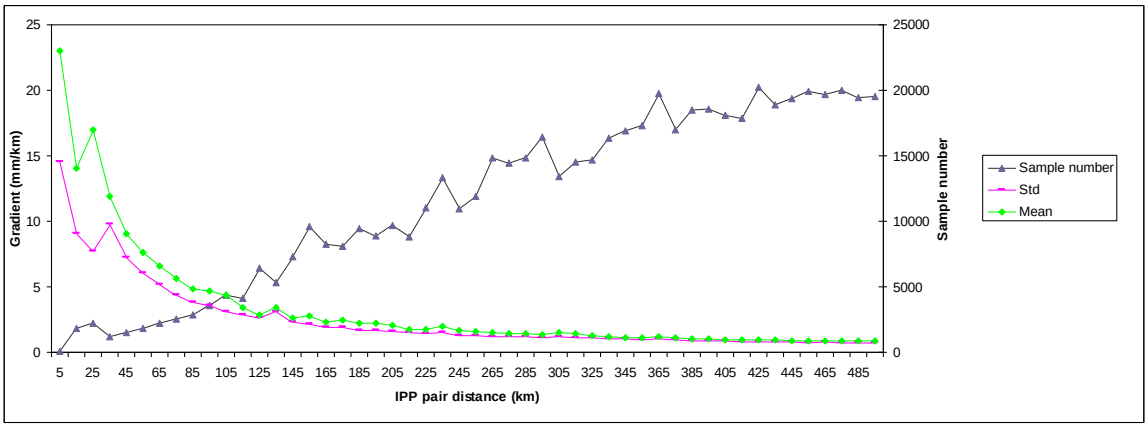

Figure 9- Mean, std and sample number per 10 km IPP separation distance bins; March 9, 2012.

Summary and conclusion

This study aimed to evaluate estimated VTEC values used for routine TEC map generation for driving nominal apparent ionospheric delay gradients in the Canadian region over quiet and moderately disturbed geomagnetic conditions. Spatial gradients studied up to a distance of 500 km revealed 95th percentile of apparent gradients exceeding 5 mm/km during moderately disturbed geomagnetic condition. Overall statistics of both apparent spatial and temporal gradients were sensitive to the level of geomagnetic activity, as given by independently derived global indices. Contribution of VTEC estimation uncertainties on the resulting spatial gradients may lead to increased gradients mainly on short distances. IPP velocity and its variability also affected resulting temporal gradients. Nonetheless this study quantified apparent gradients resulting from current VTEC estimation approaches implemented for routine TEC map generation.

References

Ciraola L., F. Azpilicueta, C. Brunini, A. Meza, and S. M. Radicella (2007). Calibration errors on experimental slant total electron content (TEC) determined with GPS. Journal of Geodesy, 81:111-120, doi: 10.1007/s00190-006-0093-1.

Ghoddousi-Fard, R., P. Héroux, D. Danskin, and D. Boteler (2011). Developing a GPS TEC mapping service over Canada. Space Weather, Vol. 9, S06D11, doi: 10.1029/2010SW00062.

Hernández-Pajares, M., J. M. Juan, and J. Sanz (2006). Medium-scale traveling ionospheric disturbances affecting GPS measurements: Spatial and temporal analysis. J. Geophys. Res., 111, A07S11, doi:10.1029/2005JA011474.

Hunsucker, R. D., and J. K. Hargreaves (2003). The high-latitude ionosphere and its effects on radio propagation. Cambridge University Press.

Jacobson, A. R., R. C. Carlos, R. S. Massey, and G. Wu (1995). Observation of travelling ionospheric disturbances with satellite-beacon radio interferometer: Seasonal and local time behaviour, J. Geophys. Res., 100, 1653-1665.

Lee, J., S. Pullen, S. Datta-Barua, and P. Enge (2006). Assessment of nominal ionosphere spatial decorrelation for LAAS. Position, Location, And Navigation Symposium, 2006 IEEE/ION, pp. 506-514, doi: 10.1109/PLANS.2006.1650638.

Sardón, E., and N. Zarraoa (1997). Estimation of total electron content using GPS data: How stable are the differential satellite and receiver instrumental biases? Radio Science, Vol. 32, No. 5, pp. 1899 – 1910.

Walter, T., S. Datta-Barua, J. Blanch, and P. Enge (2004). The Effects of Large Ionospheric Gradients on Single Frequency Airborne Smoothing Filters for WAAS and LAAS," Proceedings of ION 2004 Annual Meeting, San Diego, CA., Jan., 2004.